Modeling and Simulation of a Mechatronic Unit EOD/IEDD

L. A. Zuñiga A.*, J.C. Pedraza O., E. Gorrostieta**, M.A. Aceves**, J. M. Ramos**, J.M. Herrera R.***, C.A. Olmos****

**Secretaria de la Defensa Nacional, Av. Industria Militar, No. 1111, Col. Lomas de Tecamachalco, México (e-mail: adrian_dgim@prodigy.net.mx)*
***CIDIT-Facultad de Informática Universidad Autónoma de Querétaro,México (e-mail: carlos.pedraza@uaq.mx, juan.ramos@uaq.mx, efrengorrostieta@gmail.com, marco.aceves@uaq.mx, caolmos@uaq.mx)*
**** CIMAV*

Abstract: This paper presents a proposal for modeling and simulation of a mechatronic unit called EOD/IEDD, by carrying out a modeling and simulation of a proposed control, this unit is applied to perform hazardous-duty operations. This methodology includes the model and simulation for the behavior of a mobile manipulator with 5 degrees of freedom. The simulation considers the dynamic of system coupled, such that the errors in the model can be detected and later confined by control.

1. INTRODUCTION

This Mechatronic Unit EOD/IEDD (explosive ordinance disposal/ improvised explosive device disposal) takes the place of humans in the work of bomb detection, removal, transportation and detonation (Graham, 2006). Bombs that are difficult to neutralize or demolish because of the location may not be suitable to explode for fear of human injury or building damage. Due to this fact, it is clear the disposal operation is a big challenge for the operators especially when the surroundings are complex and cluttered (State Agency for Civil Protection, 2005).

The mobile manipulator is a multi-link arm with ability to move in a plane or space which is mounted on a vehicle (Zuñiga, 2008). These systems may have especial and important tasks such that these missions can result instability leading to overturning. Although the motion of manipulator may have universe effects on the stability of the card, because of dynamic interface between the vehicle and manipulator, the action of manipulator may be controlled to compensate the threshold of stability (Zuñiga, 2008).

In previous work, a modeling and simulation proposal for this mechatronic unit was made by considering the mobile unit and the manipulator in a separated way (Ghaffari, 2004). The present work considers the modeling and simulation of both the mobile unit and the manipulator in a coupled way; this represents more accurately the behavior of the whole robot.

The kinematics of the mechatronic unit for its orientation and steering angle along the path is derived. Next unit dynamics are derived in terms of path geometry, and the constraints on unit motions are formulated in this paper.

The stability of a mobile manipulator has a close relation with the unit's motion. In this paper, the nonlinear equations of a mobile manipulator which moves in a vertical plane have been derived.

The measure for determining the stability criterion of the mobile manipulator is the tires upward force (Bayle, 2003).

2. DEVELOPMENT OF WORK

To begin with the modeling and simulation is necessary to establish the parameters of design:

Table 1. Design Parameters

PARAMETER	AMOUNT
Max. Load	10 kg.
Speed	1.7 km/hr.
Gripper	Interchangeable
Climbing	Step according to NOM-001-STPS-1999
Long, Width, Weight.	1.7 m, 1 m, 60 kg.

2.1 Modeling and simulation methodology

In order to carry out the modeling and simulation of the mechatronic unit already mentioned (mobile unit + manipulator) it is necessary to establish the methodology to understand the behavior of the whole system. Our proposal considers the interaction among several computer tools as shown in figure 1.

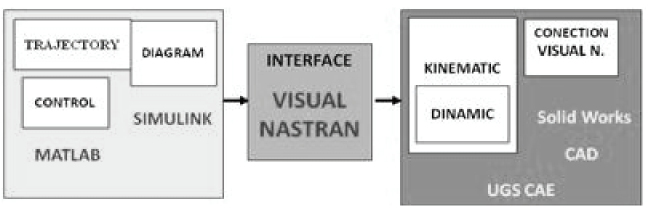

Fig. 1. Block diagram of the proposed computer tools.

Next, a modeling and simulation methodology is proposed to understand the behavior of the whole mechatronic unit, as can be seen on figure 2.

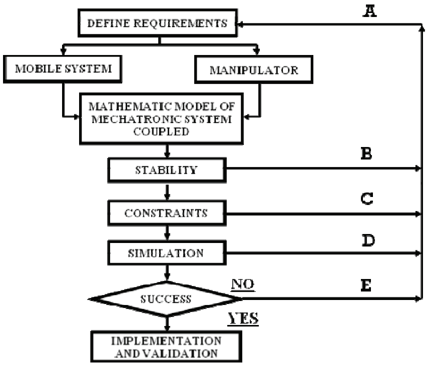

Fig. 2. Methodology proposals of M&S.

For modeling the complete system are considered two cases:

Case 1. The mobile manipulator coupled is in steady state, considering the wheels allow rotating on its axis of torso.

Case 2. The mobile manipulator coupled moves to forward, moving its arm.

First, the complete mathematical model of the manipulator coupled over a platform rotation is considered.

2.2 Direct Kinematic (case 1)

In the convention D-H, each homogeneous transformation Ei can be obtained thus (Sciavicco, 2004) (Ghaffari, 2004):

$$Ei=\begin{bmatrix} Cos(\theta_i) & -Sen(\theta_i)Cos(\alpha_i) & Sen(\theta_i)Sen(\alpha_i) & 0 \\ Sen(\theta_i) & Cos(\theta_i)Cos(\alpha_i) & -Cos(\theta_i)Sen(\alpha_i) & 0 \\ 0 & Sen(\alpha_i) & Cos(\alpha_i) & d_i \\ 0 & 0 & 0 & 1 \end{bmatrix} \quad (1)$$

Using a CAD software, the complete system is designed and obtained, as can be seen on figure 3. This manipulator has 5 pairs kinematics, which 4 are of rotation (1, 2, 4, 5) and one (3) is prismatic.

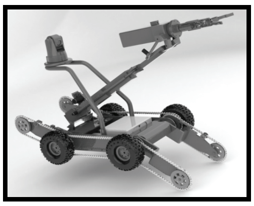

Fig. 3. Mechatronic unit.

On figure 4, the kinematics of the manipulator can be easily observed.

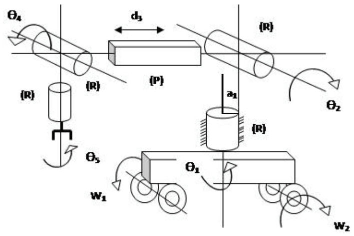

Fig. 4. Mobile manipulator's diagram.

The axis z1 has the direction R2. If we consider

$\{x_i\}= \pm((\{z_{i-1}\}\wedge\{z_i\})/|(z_{i-1}\}\wedge\{z_i\})|)$,

the α_i will be 0 or + 90^o. The parameters of mobile manipulator are shown in the next table:

Table 2. Denavit-Hartenberg parameters

I	Var	α_i	a_i	d_i	cos α_i	sin α_i	(fig.) Θ_i
1	θ_1	90º	a_1	d_1	0	1	0º
2	θ_2	90º	0	d_2	0	1	90º
3	θ_3	0º	0	d_3	1	0	0º
4	θ_4	90º	0	0	0	1	270º
5	θ_5	0º	0	0	1	0	0º

The transformation matrix is T_5:

$$\begin{bmatrix} c_1c_2c_4c_5+s_1s_4c_5+c_1s_2s_5 & -c_1c_2c_4s_5-s_1s_4s_5+c_1s_2c_5 & c_1c_2s_4-s_1c_4 & c_1s_2d_3+s_1d_2+a_1c_1 \\ s_1c_2c_4c_5-c_1s_4c_5+s_1s_2s_5 & -s_1c_2c_4s_5+c_1s_4s_5+s_1s_2c_5 & s_1c_2s_4+c_1c_4 & s_1s_2d_3-c_1d_2+a_1s_1 \\ s_2c_4c_5-c_2s_5 & -s_2c_4s_5-c_2c_5 & s_2s_4 & -c_2d_3+d_1 \\ 0 & 0 & 0 & 1 \end{bmatrix} \quad (2)$$

The origins of system reference unite to hand to be denoting for the vector $\{p\}$. For the vector of hand orientation the reference to axis $\bar{z}$ to be nominate approximate vector $\{a\}$. The reference to axis $\bar{y}$ is the orientation vector $\{s\}$; your direction is the union the finger of the holding hand. For the $\bar{x}$ axis, it is the normal vector $\{n\}$, therefore (Ghaffari, 2004) (Lewis, 1993): $\{n\}=\{s\}\wedge\{a\}$;

$$T_0^5=\begin{bmatrix} R_0^5 & d_0^5 \\ 0 & 1 \end{bmatrix} \quad (3)$$

Where R_0^5 Є R^{3x3} is the orientation 0_5 X_5 Y_5 Z_5 relative to inertial base 0_0 X_0 Y_0 Z_0. d_0^5 Є R^3 denote the position vector or translation of griper reference to inertial base, 0 = [0 0 0] is denote the perspective transformation and 1 is the scaling factor (Ghaffari, 2004).

2.3 Inverse Kinematic (case 1)

In this manipulator, the vector {p} can be defined in the last column of $[T_5]$, that is:

$$\begin{Bmatrix} p_x \\ p_y \\ p_z \end{Bmatrix} = \begin{Bmatrix} c_1s_2d_3+s_1d_2+a_1c_1 \\ s_1s_2d_3-c_1d_2+a_1s_1 \\ -c_2d_3+d_1 \end{Bmatrix} \quad (4)$$

Substituting the value of the equation and finally, obtain T1 or the angle θ_1:

$$\theta_1 = \operatorname{arctg}\left[\frac{\pm\sqrt{p_x^2 + p_y^2 - d_2^2 - a_1^2} * p_y + p_x d_2}{\pm\sqrt{p_x^2 + p_y^2 - d_2^2 - a_1^2} * p_x - p_y d_2}\right] \quad (5)$$

The orientation of the hand to be defining as the angle of balancing, Θ, around of axis z, of pitching, Φ, around of axis *y* and of yaw, Ψ, around of axis x. the formulate show the form of obtain the rotation matrix (Sciavicco, 2004) (Ghaffari, 2004):

$$[T] = [R_{\psi\phi\theta}] = [R_{\theta,z}][R_{\phi,y}][R_{\psi,x}] \quad (6)$$

Considering the Θ angle to be defined, and due the signs of quotient, the angle Φ is

$$\Phi = \operatorname{arctg}\left[\frac{-n_z}{n_x \cos\theta + n_y \operatorname{sen}\theta}\right] \quad (7)$$

$$\Psi = \operatorname{arctg}\left[\frac{a_y \operatorname{sen}\theta - a_y \cos\theta}{-s_x \operatorname{sen}\theta + s_y \cos\theta}\right] \quad (8)$$

2.4 Differential Kinematic (case 1)

If [T] is the matrix of transformation that shown the position and orientation of manipulator hand, the new matrix will be:

$$J_{vi} = z_{i-1} x (o_n - o_{i-1}); \qquad J_{vi} = z_{i-1}$$

$$J = \begin{bmatrix} z_0 x(o_5 - o_0) & \dots & z_3 x(o_5 - o_2) & \dots & z_4 x(o_5 - o_4) \\ z_0 & z_1 & 0 & z_3 & z_4 \end{bmatrix} \quad (9)$$

Note that the joint 3 is prismatic:

$$o_3 = o_4 = \begin{bmatrix} c_1 s_2 d_3 + s_1 d_2 + a_1 c_1 \\ s_1 s_2 d_3 - c_1 d_2 + a_1 s_1 \\ -c_2 d_3 + d_1 \end{bmatrix} \quad (10)$$

We use the homogeneous transformation matrix to determine O_0, O_1, O_5; as well as the corresponding vector z_i.

2.5 Mobile manipulator (case 2)

Po Intersection of the axis of symmetry with the driving wheel axis
Pc Center of mass of the platform;
Pb Location of the manipulator on the platform
Pr Reference point to be followed by the mobile platform
B Distance between the driving wheels and the axis of symmetry
r Radius of each driving wheel
mc Mass of platform without the driving wheels and motors
mw Mass of each driving wheel plus motors
Ic Moment of inertia of the motors about a vertical axis through Po
Iw Moment of inertia of each wheel and the motor about the wheel axis;
Im Moment of inertia of each wheel and the motor about the wheel diameter.

Instantaneous center of rotation (ICR) or instantaneous center of curvature (ICC) is a cross point of all axes of the wheels (Bayle, 2003) (Yamamoto, 1994) with mobility degree 2 and degree of steereability 0.

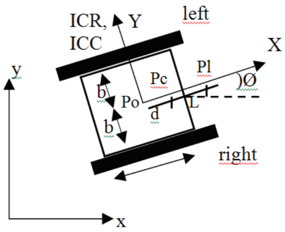

Fig. 5. Diagram of mobile platform

$$q = (x_c, y_c, \phi, \theta_r \theta_l) \quad (11)$$

Three variables (x_c, y_c, ϕ) describe the position and orientation of the platform. Two variables specify the angular positions for the driving wheels (Korayem, 2004).

Adding non-holonomic constraints

1. Is that the platform must move in the direction of the axis of symmetry (holonomic).

$$\dot{y}_c \cos\phi - \dot{x}_c \sin\phi - d\dot{\phi} = 0 \quad (12)$$

2. Are the rolling constraints, not slip (nonholonomic).

$$\dot{x}_c \cos\phi + \dot{y}_c \sin\phi + b\dot{\phi} = r\dot{\theta}_r \quad (13)$$

$$\dot{x}_c \cos\phi + \dot{y}_c \sin\phi - b\dot{\phi} = r\dot{\theta}_l \quad (14)$$

The Mobile platform's equation of motion is described by:

$$M(q)\ddot{q} + V(q,\dot{q}) = E(q)\tau - A^T(q)\lambda \quad (15)$$

$M(q)$ N x N inertia matrix
$V(q,\dot{q})$ N x 1 vector of position and velocity dependent forces
$E(q)$ N x r input transformation matrix
τ r-dimensional input vector
m_c N x N inertia matrix
m_w N x 1 vector of position and velocity dependent forces
$E(q)$ N x r input transformation matrix
τ r-dimensional input vector

$$M(q) = \begin{bmatrix} m & 0 & -m_c d \sin\phi & 0 & 0 \\ 0 & m & m_c d \cos\phi & 0 & 0 \\ -m_c d \sin\phi & m_c d \cos\phi & I & 0 & 0 \\ 0 & 0 & 0 & I_w & 0 \\ 0 & 0 & 0 & 0 & I_w \end{bmatrix} \quad (16)$$

$$m = m_c + 2m_w, \qquad I = I_c + 2m_w(d^2 + b^2) + 2\,\mathrm{Im}$$

$$V(q,\dot q) = \begin{bmatrix} -m_c d\dot\phi^2 \cos\phi \\ -m_c d\dot\phi^2 \sin\phi \\ 0 \\ 0 \\ 0 \end{bmatrix}$$

$$E(q) = \begin{bmatrix} 0 & 0 \\ 0 & 0 \\ 0 & 0 \\ 1 & 0 \\ 0 & 1 \end{bmatrix} \tag{17}$$

2.6 Dynamic model of a mechatronic unit (case 2)

In this section, a mechatronic unit with ability to move in a vertical plane which is mounted on a 4-wheeled vehicle is considered. Because of the especial task of the mobile manipulator, the path of mechatronic unit and the desired task of the end-effector are predefined. Thus there are some limited configurations of manipulator while moving along its desired path. These arrangements of manipulator do not satisfy the stability criterion when the upward force of each tire tends to zero. The schematic picture of a redundant manipulator with attached coordinates to its links is shown in figure 6. The free body diagram of the mechatronic unit coupled is also shown in this figure.

By using the Denavit-Hartenberg notation (Nwokah, 2002), it is feasible to find the kinematic equations of the mobile manipulator. The Denavit-Hartenberg parameters and variables are shown in Table 2. It is assumed that the system is at the steady state condition where its unit velocity is constant.

Table 3. Denavit-Hartenberg variables

I	α_{i-1}	a_{i-1}	d_i	θ_{i-1}
1	0	a	0	0
2	0	0	0	θ_1
3	0	L_1	0	θ_2
4	0	L_2	0	θ_3
5	0	L_3	0	0

In Table 3, the first row relates the inertial coordinate to the body coordinate attached to the common point of the manipulator and unit (this row is optional). The fifth row is a pure translation that transforms the frame 4 to the frame 5. The forces and torques equations in x-y plane are as follows:

$$F_{y1} + F_{y2} + F_{y3} + F_{y4} + f_y - Mg = ma_y \tag{18}$$

$$b(F_{y2} + F_{y4}) + (-Mg + f_y + ma_y)\frac{b}{2} - hf_x + M_z - \frac{h}{2}ma_x = 0 \tag{19}$$

Assuming that the vehicle of mobile manipulator is symmetric with respect to x-y plane, it is clear that the forces Fy1 and Fy3 are equal and also Fy2 is equal to Fy4 Considering the unit at the steady state conditions, where velocities at different directions are constant, we have:

The kinematic equations may be found by using the Denavit-Hartenberg parameters from table 1 and the general transformation matrices.

By multiplying sequentially the transformation matrices from the initial frame to the end-effector frame, the kinematic equations may be found as follows:

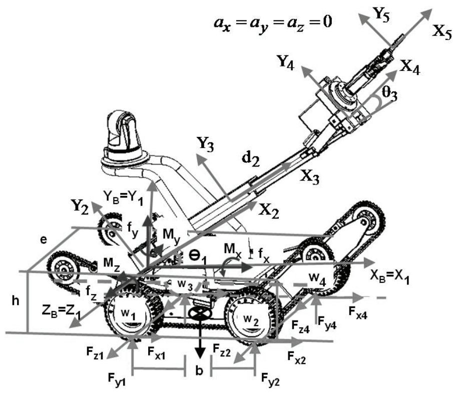

Fig. 6. Schematic diagram of mechatronic unit

$$^{i-1}_{\ i}T = \begin{bmatrix} C\theta_i & -S\theta_i & 0 & a_{i-1} \\ S\theta_i C\alpha_{i-1} & C\theta_i C\alpha_{i-1} & -S\alpha_{i-1} & -S\alpha_{i-1} d_i \\ S\theta_i S\alpha_{i-1} & C\theta_i S\alpha_{i-1} & C\alpha_{i-1} & C\alpha_{i-1} d_i \\ 0 & 0 & 0 & 1 \end{bmatrix} \tag{20}$$

$$P_x = a + L_1\cos(\theta_1) + L_2\cos(\theta_1 + \theta_2) + L_3\cos(\theta_1 + \theta_2 + \theta_3) \tag{21}$$

$$Py = L_1\sin(\theta_1) + L_2\sin(\theta_1 + \theta_2) + L_3\sin(\theta_1 + \theta_2 + \theta_3) \tag{22}$$

The velocities and acceleration equations of the end-effector can also be determined by differentiating from equations (21) and (22) with respect to time.

Therefore, for solving the inverse kinematics of the system, two equations for the position of the end-effector in the x-y plane, two equations for speed of the end-effector are employed. These are further to the two equations for the acceleration of the end-effector which are zero in this work.

The 9 variables are; $\theta_1, \theta_2, \theta_3$ for angular positions, $\dot\theta_1, \dot\theta_2, \dot\theta_3$ for angular velocities and $\ddot\theta_1, \ddot\theta_2, \ddot\theta_3$ for angular accelerations, respectively. Subsequently, the method for determining the 9 unknown variables with 6 equations will be discussed.

For optimal stability of the mobile manipulator, the summation of tires upward forces Fy1, Fy3 should be set equal to the summation of forces Fy2 and Fy4. This leads us to define a performance index to be at its minimum value during the motion of mobile manipulator.

This performance index can be set equal to the torque exerted on the first joint of manipulator attached to the unit. This equation is calculated by Lagrangian method and its accuracy is checked with the Newton- Euler iteration technique (Nwokah, 2002). The torque acting on the first joint attached to the unit is as equation (23).

The mechanic design was carried out in CAD-CAE software to analyze the tolerance adjust it to manufacture (Jackey, 2002). The Figures 8 and 9 show the block diagram and simulations results of tracking trajectory.

$$\begin{aligned} T_1 &= m_1 L_1^2 \ddot{\theta}_1 + m_2 L_1^2 \ddot{\theta}_1 + m_2 L_2^2 (\ddot{\theta}_1 + \ddot{\theta}_2) + 2 m_2 L_1 L_2 c_2 \ddot{\theta}_1 \\ &+ m_2 L_1 L_2 c_2 \ddot{\theta}_2 + m_3 L_1^2 \ddot{\theta}_1 + m_3 L_2^2 (\ddot{\theta}_1 + \ddot{\theta}_2) + m_3 L_3^2 (\ddot{\theta}_1 + \\ &\ddot{\theta}_2 + \ddot{\theta}_3) + 2 m_3 L_1 L_2 c_2 \ddot{\theta}_1 + m_3 L_1 L_2 c_2 \ddot{\theta}_2 + 2 m_3 L_1 L_3 c_{23} \ddot{\theta}_1 \\ &+ m_3 L_1 L_3 c_{23} \ddot{\theta}_2 + m_3 L_1 L_3 c_{23} \ddot{\theta}_3 + 2 m_3 L_2 L_3 c_3 \ddot{\theta}_1 + 2 m_3 L_2 \\ &L_3 c_3 \ddot{\theta}_2 + m_3 L_2 L_3 c_3 \ddot{\theta}_3 - 2 m_3 L_1 L_2 s_2 \dot{\theta}_1 \dot{\theta}_2 - m_3 L_1 L_2 s_2 \dot{\theta}_1^2 - \\ &2 m_3 L_1 L_3 s_{23} \dot{\theta}_1 (\dot{\theta}_2 + \dot{\theta}_3) - m_3 L_1 L_3 s_{23} \dot{\theta}_2 (\dot{\theta}_2 + \dot{\theta}_3) - m_3 L_1 L_3 \\ &s_{23} \dot{\theta}_3 (\dot{\theta}_2 + \dot{\theta}_3) - 2 m_3 L_2 L_3 s_3 \dot{\theta}_1 \dot{\theta}_3 - 2 m_3 L_2 L_3 s_3 \dot{\theta}_2 \dot{\theta}_3 - m_3 L_2 \\ &L_3 s_3 \dot{\theta}_3^2 + m_1 g L_1 c_1 + m_2 g L_1 c_1 + m_2 g L_2 c_{12} + m_3 g L_2 c_{12} + m_3 \\ &g L_2 c_{12} + m_3 g L_3 c_{123} - 2 m_2 L_1 L_2 s_2 \dot{\theta}_1 \dot{\theta}_2 - m_2 L_1 L_2 s_2 \dot{\theta}_2^2 \end{aligned} \qquad (23)$$

2.7 Mobile manipulator's Simulation (case 2)

The basic properties of the dynamic model are (Sciavicco, 2004) (Lewis, 1993):

$$M(q)\ddot{q} + C(q,\dot{q})\dot{q} + G(q) = \tau \qquad (24)$$

- Linearity in the dynamics parameters.
- Inertia Matrix, M(q)
- Centrifuge Matrix and Coriolis, C(q, qp)
- Gravity vector, G(q)
- Dynamic residual, H(eq, eqp)
- τ is the Torque Control.

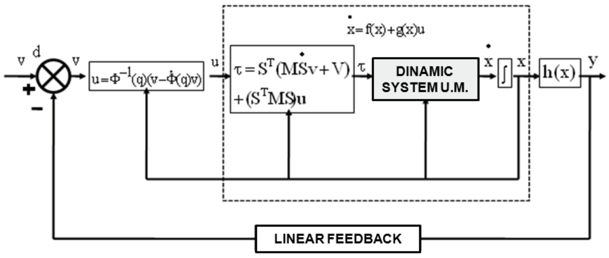

Fig. 7. System block diagram.

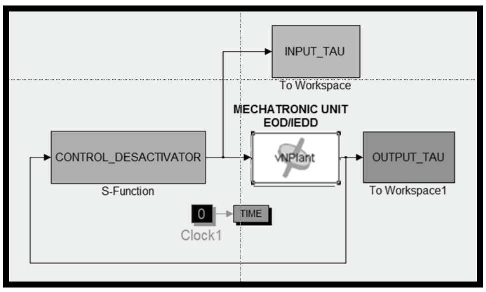

Fig. 8. System block diagram.

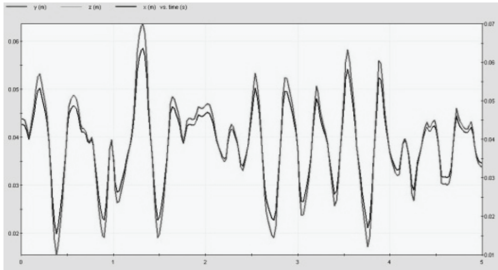

Fig. 9. Tracking of trajectory in visual nastran.

The compensated mobile manipulator, the performance index has a value less than 1 N-m which is well below than the uncompensated mobile manipulator when considered informally for some states of system through motion. It can be expected from this system when the dynamic interaction between the vehicle and manipulator would not exist, the two tire upward forces could be exactly equal to each other. Even though despite existence of those dynamical effects, it can rely on that the mobile manipulator is able to move safely without overturning.

Therefore the Performance index for a specific case of mobile manipulator when v = 1(m / s), b = 0.5(m),α = 0.5(rad).

The design criterion was to control the mobile platform so that the manipulator is maintained at a configuration which maximizes the manipulability measure. We could use the desired path to feed back the error (Yamamoto, 1994) (Korayem, 2004) (Nwokah, 2002)

$$e = y^d - y, \quad \ddot{y} = v = \ddot{y}^d + K_d(\dot{y}^d - \dot{y}) + K_p(y^d - y) \qquad (25)$$

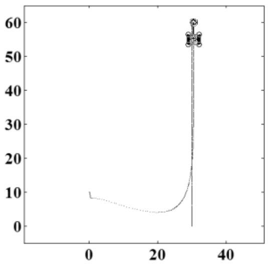

Fig. 10. Tracking of trajectory ideal against real.

Next, the task is to use the CAD model to generate motion during 5 time constants. By using a build matlab function (ode45) for the simulation process, it took 5 seconds to stabilize.

2.8 Results and Validation.

The gripper has a form seem to hand-human with motions shown in figure 11.

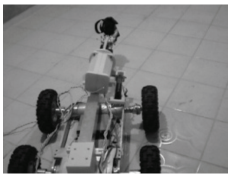

Fig. 11. Cad with Open and roll of gripper.

The torque to close of gripper is given by:

$$\mu \; nf \; Fg = w \; g \qquad (26)$$

Where:

μ: Constant of friction, nf: Number of finger in contact.
Fg: Force of gripper. g: Gravity force g=3; due to loads dynamics. (sf)

The validation of mechanic structure is done by CAE software applying the analysis for element finite (fem) (Nwokah, 2002), manufacturing the parts by aluminum 6061-T6, to load of 10 kg.

6. CONCLUSIONS

The methodology proposed for modelling and simulation showed reasonable results. Also, the virtual rapid prototyping of the robot for the load and the mechanic system was validated. In addition, the simulations displayed using a solid model, in such way that an engineer can observe the simulated motion system response were shown. Furthermore, dynamics and simulation environments were easily changed in either the simulation or the control algorithm. This facilitated the testing by modifying certain parameters of the robot.

As future work, the full development of a methodology of modelling and simulation applied to a mechatronic unit eod/iedd is considered to test and validate several control techniques

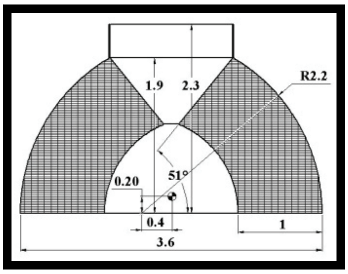

Fig. 12. Workspace of mobile robot.

Table 4. Prototype parameters.

Features	Parameters
Dimensions	90 cm width, 170 cm long and Scope to high of 2 metros.
Feed	24 v, 18 amp-hr. (3 hours of autonomy).
Motors CD	2 servomotors, 1 motor permanent imam, 10 linear actuators.
Locomotion	2 wheels driving y 2 wheels more, Skid steer type.
Manipulator	1 manipulator of configuration type Stanford of 5 degree freedom.
Speed	1.7 km/hr.
Gripper	Pitch: 90°, Roll: 360° and Press: 100°

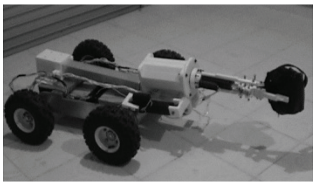

Fig. 13. Final prototypes in tests.

REFERENCES

Ali Ghaffari, Ali Meghdari, Davood Naderi and Sohrab Eslami (2004). "International Journal of Advanced Robotic Systems", in *Stability enhancement of mobile manipulators via soft computing,* Vol. 12, No. 3, pp. 191-198.

A. Jackey Robyn (2002), *Virtual Robot Prototyping and Control*, Clarkson University, USA, November 2002, pp. 1-10.

B. Bayle, J-Y. Fourquet and M. Renaud (2003). "Journal of Intelligent and Robotic Systems," in *Nonholonomic Mobile Manipulators: Kinematics, Velocities and Redundancies* vol. 36, January 2003, pp. 45 – 63.

F. L. Lewis, C. T. Abdallah, D. M. Dawson (1993), *Control of Robot Manipulators*, Editorial Maxwell McMillan, Canada, pp. 25-36.

J. J. Craig (2006), *Robotica*, Editorial Pearson Prentice Hall, México, pp. 36-90.

L.A. Zuñiga A. and J.C. Pedraza O. (2008). "Emerging Technologies, Robotics and Control Systems.", in *Modeling and Simulation of a Mobile Robot applied to the manipulation of Explosives*, pp. 48-54.

L. Sciavicco and B. Siciliano (2004). *Modelling and Control of Robot Manipulators*, Ed. Springer-Verlag, pp. 15-20.

M. H. Korayem, T. Banirostam (2004). "3rd IFAC Symposium on Mechatronic Systems", in *Design, Modeling and Experimental Analysis of Wheeled Mobile Robots,* 2/a. ed. Vol. 12, September 2004, pp. 821-228.

O. Nwokah and Y. Hurmuzlu (2002). *The Mechanical Systems Design Handbook,* Southern Methodist University Dallas, Texas, 2002, pp. 458-550.

State Agency for Civil Protection (2005). *Specification of Tools and Devices for the Bomb Disposal and Rescue System,* California, U.S.A., 2005, pp. 30-100.

T. Graham (2006). *Bombs and Bombings,* Illinois, U.S.A., pp. 58-130.

Y. Yamamoto and X. Yun (1994). "IEEE Transactions on Automatic Control," in *Coordinating Locomotion and Manipulation of a Mobile Manipulator,* 6/a ed. vol. 39, June 1994, pp. 1326-1332.